Chinese Chemical Letters 34 (2023) 107700

Contents lists available at ScienceDirect

Chinese Chemical Letters

journal homepage: www.elsevier.com/locate/cclet

Detection of avian influenza virus H9N2 based on self-driving and self-sensing microcantilever piezoelectric sensor

Yawen Zhang[1], Feng Shi[1], Chenguang Zhang, Xin Sheng, Yunhao Zhong, Hui Chong, Zhanjun Yang*, Chengyin Wang*

College of Chemistry and Chemical Engineering, Yangzhou University, Yangzhou 225002, China

ARTICLE INFO

Article history:
Received 18 March 2022
Revised 4 July 2022
Accepted 21 July 2022
Available online 24 July 2022

Keywords:
Micro cantilever sensor
Self-driving
Self-sensing
Piezoelectric material
Avian influenza virus H9N2

ABSTRACT

In this article, we used the self-excitation and self-inductance characteristics of polyvinylidene fluoride (PVDF) piezoelectric materials, combined with the powerful signal processing and calculation analysis capabilities of integrated circuits, for the first time to explore a set of microcantilever sensor "readout system" without additional driver (self-driving) and can realize self-sensing external signal (self-sensing). It was successfully applied to the unlabeled detection of avian influenza virus (AIV) H9N2. The specific force of the antigen-antibody complexes on the surface of the microcantilever leads to the change of the stress of the cantilever, which drives the constructed detection device, and does not require an additional excitation source to drive it, that is, the self-driving part. At the same time, due to the movement of piezoelectric charges in the film caused by the positive piezoelectric effect of the PVDF film, self-inductive charges are generated on the surface of the sensor dielectric. The charge signal is converted into a voltage signal, and the sensing part is completed, that is, self-sensing. The immunosensor has a linear range of 100-1000 ng/mL with a detection limit of 2.9 ng/mL. The method will also open up a new avenue for the detection of other analytes based on antigen-antibody responses.

Avian influenza virus (AIV) was first found in sick turkeys in 1996. It has attracted extensive attention all over the world because of its high infectivity and mortality. The outbreak of influenza virus every year poses a great threat to people's economy and health. According to previous reports, H9N2 can be transmitted between animals and humans, indicating H9N2 as a potential hazard [1,2]. Traditional virus related detection methods usually include virus isolation and culture, serological test, polymerase chain reaction (PCR), enzyme-linked immunosorbent assay (ELISA), *etc.* [3,4]. Although these methods have high sensitivity, they are not suitable for real-time virus detection because of long analysis time, high detection cost and the need for professional operators. Therefore, it is of great practical value to develop a quantitative, highly sensitive, simple and cheap method for virus detection.

In recent years, biosensors have been widely used in biological detection [5,6]. Biosensors based on microcantilever have attracted much attention because of their miniaturization, label free detection and high sensitivity [7–9]. Generally, microcantilever can be used as both microbalance and surface stress sensor. The former realizes the detection by measuring the shift of resonance frequency caused by the change of mass before and after surface adsorption of target molecules; The latter is realized by detecting the bending deformation of the cantilever beam in the biochemical reaction [10–12]. All microcantilever sensors are equipped with a readout device that can measure the mechanical response of the system. There are many traditional readout systems, among which the measurement based on optical method is the most commonly used. The researchers of our research group successfully achieved the quantitative detection of H9N2 virus *via* the micro cantilever sensor based on optical detection [13]. Maruyama *et al.* reported a cantilever surface stress sensor based on optical interferometry to achieve the detection of human serum albumin [14]. Although the detection technology based on optics is very sensitive, it also has some limitations, mainly including high cost, large volume and high surface treatment requirements. The piezoelectric method (that is, a layer of piezoelectric material is adhered to the cantilever surface. When the cantilever is bent and deformed, the piezoelectric layer will produce induced charge, and the bending deformation of the micro cantilever is reflected by measuring the induced charge). With the advantages of high sensitivity, fast response, low cost and easy circuit integration, it has become a new field of micro cantilever sensor research [15].

* Corresponding authors.
E-mail addresses: zjyang@yzu.edu.cn (Z. Yang), wangcy@yzu.edu.cn (C. Wang).
[1] These authors contributed equally to this work.

https://doi.org/10.1016/j.cclet.2022.07.043
1001-8417/

At present, the reports on piezoelectric microcantilever biosensors only focus on self-driven micro cantilever sensors or self-sensing microcantilever sensors. "Self-driving" means that materials do not need to be driven by external excitation conditions (such as electricity, heat, light, magnetic field and sound wave), but mainly based on spontaneous physical or chemical processes of materials [16]; "self-sensing" refers to the ability of materials to perceive their own state (such as stress, strain and temperature), and transmit dynamic information in real time without additional sensors [17,18]. Zhou *et al.* first reported the detection of freon gas using self-driven piezoelectric micro cantilever as a mass sensitive sensor [19]. Faegh research group used ZnO as piezoelectric material to prepare self-sensing micro cantilever sensor to detect glucose molecules with different concentrations [20,21]. However, there is no report on the construction of micro cantilever sensor with self-driving and self-sensing characteristics and its application in biological/chemical measurement system. Therefore, we hope to develop a sensor device with self-driving and self-sensing characteristics.

Polyvinylidene fluoride (PVDF) is a kind of piezoelectric polymer, which has the advantages of large piezoelectric constant (under the same external load condition, the voltage is more than ten times that of piezoelectric ceramics), light, thin, soft and easy to process into any shape. Therefore, we choose PVDF piezoelectric film as the sensing element, and establish a sensor with self-driving and self-sensing characteristics through self-made circuit, analog-to-digital converter, demo board and the personal computer (PC) detection program. When the stress on the cantilever surface changes, the voltage signal can be obtained. The antigen antibody specific force changes the surface stress of the cantilever and drives the constructed detection device without additional excitation conditions, that is, the self-driving part; at the same time, due to the positive piezoelectric effect of the piezoelectric film, the self-induced charge is generated on the sensor surface. Through the analog-to-digital converter and the demo board, the charge signal is transformed into voltage signal output, and the sensing part is completed, that is, the self-sensing part.

In addition, nano materials have the advantages of large specific surface area and easy surface modification, which are helpful to fix more signal probes. In recent years, nano materials have become a common method to improve the sensitivity of biosensors [22,23]. UiO-66-NH_2 is a classic Zr-based metal-organic framework (MOF), which can be used as an excellent carrier for the immobilization of biomolecules due to its advantages of large specific surface area, simple function, and good stability. In addition to this, they can also serve as carriers for the deposition of metal nanoparticles and other species [24,25]. Because of its large specific surface area and good biocompatibility, Au nanoparticles (AuNPs) can be used as a good substrate material for immobilizing biomolecules and amplifying the detection signal [26]. The sensitivity of microcantilever sensor is improved by double signal amplification of UiO-66-NH_2 and AuNPs. The essence of signal amplification of nanomaterials is that its larger specific surface area leads to an increase in the adsorption amount of the measured object [27]. UiO-66-NH_2 has a large specific surface area, and the amino group on its surface can connect more AuNPs, and AuNPs can bind to antibodies by Au-N bond. In addition, the carboxyl group on the surface of UiO-66-NH_2 can form an amide bond with the amino group on the surface of the antibody to bind the antibody, thus achieving double signal amplification [28,29]. Therefore, we amplified the signal through AuNPs/UiO-66-NH_2 nano materials and modified the H9N2 antibody on one side of the micro cantilever. The specific reaction of antigen antibody changed the surface stress of the cantilever, thus changing the output voltage of the sensor, and established the relationship between H9N2 concentration and the output voltage of the sensor.

The materials, apparatus, and the preparation of nanomaterials are described in Supporting information.

The structural diagram of PVDF piezoelectric film is shown in Fig. S1a (Supporting information). From top to bottom, there are upper surface silver layer, PVDF piezoelectric layer, lower surface silver layer and PET polyester sheet (used to protect the lower surface silver layer).

The processing steps of the experimental sensor are as follows: (1) spray gold on the upper surface of the sensor, which can be used for protecting the electrode on the one hand and functional modification on the other hand; (2) take a 5 cm Farrow Cable double core shielded wire (to prevent external static electricity from interfering with the sensor signal), remove the 5 mm skin at both ends, and then weld the two inner core wires at one end with the pins on the upper and lower surfaces of the sensor, and the other end with PH 2.0 terminal wire. In order to facilitate subsequent experiments, the upper surface is connected with black wire and the lower surface is connected with red wire by default; (3) wrap parafilm sealing film around the welding position for fixation, while preventing mutual contact between electrodes. The fabricated sensor is shown in Fig. S1b (Supporting information).

The test cell consists of two parts: sealing ring (hollow area of 10×11 cm) and base (Fig. S1c in Supporting information); first, apply phenolic epoxy resin evenly on the surface of the sealing ring, then cover the sensor on it. (Fig. S1d in Supporting information, the hollow position is the sensing part). After the glue is cured, apply phenolic epoxy resin around the sealing ring, push the sensor and the sealing ring into the base, and apply phenolic epoxy resin at the interface for sealing (Fig. S1e in Supporting information).

The schematic illustration of the fabrication of the proposed microcantilever sensor was shown in Fig. 1. The previously fabricated microcantilever sensor is washed with absolute ethanol and deionized water, dried with nitrogen, and then placed in a sealed bag for storage. AuNPs/UiO-66-NH_2 nanoparticles dispersion (7 mg/mL) was dropped on the sensor surface and dried at room temperature. Add 1-(3-dimethylaminopropyl)-3-ethylcarbodiimide hydrochloride/*N*-hydroxy succinimide (EDC/NHS) mixture dropwise, wait for 1 h, and then rinse the sensor surface with PBS. H9N2 antibody was dropped onto the surface of the sensor and placed at 4 °C for 12 h. After removal, the microcantilever sensor was washed with PBS, and then sealed with 1% BSA. Finally, the modified micro cantilever sensor was stored at 4 °C.

The microcantilever sensor processed above is connected with analog-to-digital converter and demo board through self-made circuit, and connected with PC through USB cable to enter the operation interface of Arduino software and input the corresponding detection code (Fig. 2). Adding 100 μL different concentration standard solutions containing H9N2 antigen fragments on the microcantilever sensor, when immune reaction occurs between antigen and antibody, specific force is generated, which changes the stress on the upper and lower surfaces of the micro cantilever, resulting in the increase of output voltage. We can detect H9N2 antigen with high sensitivity by recording the voltage changes generated by antigen solutions with different concentrations through Arduino software, to establish the relationship between antigen solution concentration and output voltage. The sensor proposed by us does not need external power supply, but relies on the voltage generated by the stress change of the piezoelectric film to realize the self-driving and self-sensing detection of H9N2.

Figs. 3a and b displayed the SEM and TEM images of UiO-66-NH_2/AuNPs. SEM images show that the crystal structure of UiO-66-NH_2 presents octahedral geometry with an average size of 100 nm. As Fig. 3b shows, a large number of Au particles are attached to the surface of UiO-66-NH_2, indicating the successful preparation of UiO-66-NH_2/AuNPs. The crystal structure of UiO-66-NH_2

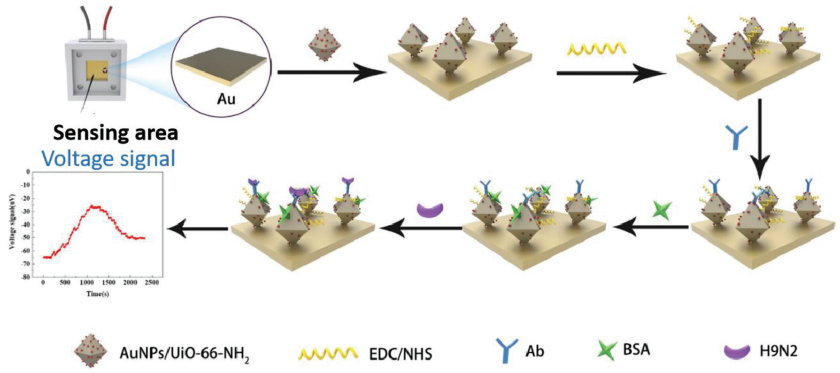

Fig. 1. Schematic diagram of preparation process of micro cantilever immunosensor.

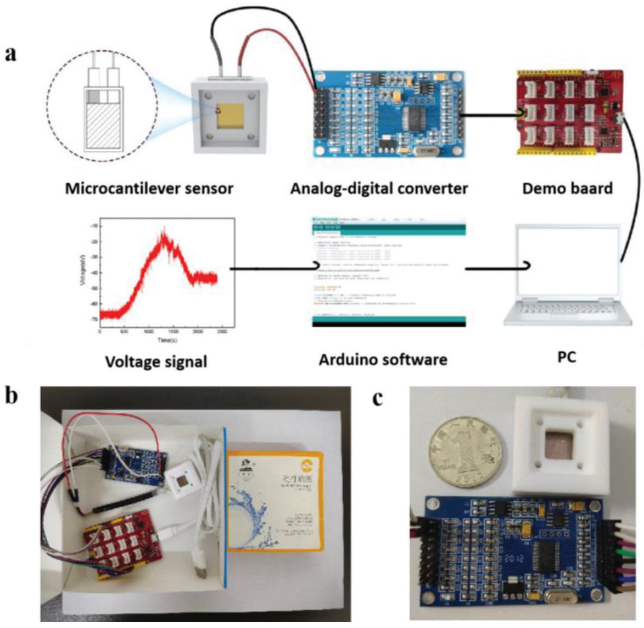

Fig. 2. (a) Schematic diagram of detection platform. (b) Comparison between actual detection device and qualitative filter paper. (c) Comparison between actual detection device and an one yuan coin.

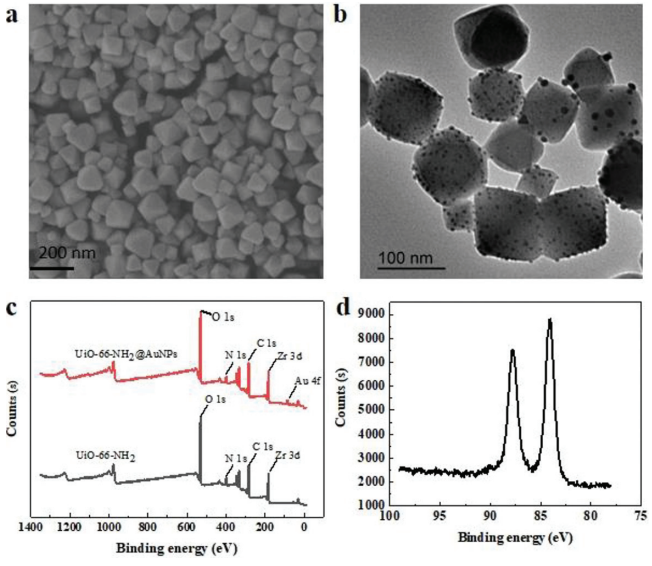

Fig. 3. (a) SEM of UiO-66-NH_2. (b) TEM of UiO-66-NH_2/AuNPs. (c) XPS of UiO-66-NH_2/AuNPs and (d) the Au 4f region.

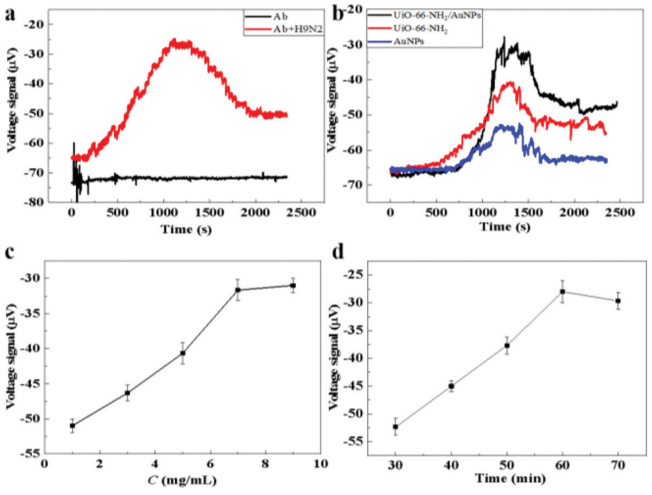

Fig. 4. (a) Voltage response of microcantilever sensor to H9N2. (b) Comparison of sensor signal amplification effects. (c) Optimization of UiO-66-NH_2 concentration, and (d) the EDC/NHS activation time.

and AuNPs/UiO-66-NH_2 composites were further characterized by XRD. Fig. S2 (Supporting information) shows the XRD pattern of the sample. It can be seen that UiO-66-NH_2 is consistent with the results reported in the literature [30]. The resultant Zr-based MOF presents three typical diffraction peaks at 4.8° (111), 7.1° (002), and 12.1° (022), which support the cubic configuration of the sample [30]. The diffraction peaks at 17.08° (400), 19.16° (420), 22.38° (511), 25.18° (600), and 30.88° (640) the octahedral geometry (JCPDF card number: 36-1452), indicating the octahemioctahedral crystal structure of the MOF materials [31]. In the AuNPs/UiO-66-NH_2 composites, a new single metallic Au peak appears. There are four characteristic peaks of Au at 38.18° (111), 44.4° (200), 64.58° (220) and 77.55° (311) [32]. These results also show that the Au nanoparticles overlap intensively on the MOFs, thus isolating the XRD signals of the MOFs. In addition, XPS was performed for the investigation of elemental analysis of UiO-66-NH_2/AuNPs. As shown in Fig. 3c, the fully scanned spectra suggested the existence of carbon, nitrogen, oxygen, gold, and zirconium elements in UiO-66-NH_2/AuNPs. The Au4f (Fig. 3d) indicate the existence of the Au. According to the results of elemental analysis, the formation of UiO-66-NH_2/AuNPs was further confirmed.

Fig. 4a is a voltage response signal of a microcantilever sensor modified with H9N2 antibody by injecting a certain concentration of antigen into the surface of the microcantilever sensor modified with H9N2 antibody and only H9N2 antibody. As can be seen from Fig. 4a, after the antigen solution is injected, the voltage value continues to increase and does not return to the initial voltage. This

is because after dropping a certain concentration of H9N2 antigen, the surface stress of the microcantilever is changed due to the specific reaction of antigen antibody, which leads to the change of the output voltage of the cantilever.

In order to investigate the effect of nanomaterials on the voltage signal of the sensor, we investigated the voltage signal value of the sensor when using AuNPs, UiO-66-NH_2 and AuNPs/UiO-66-NH_2 materials to immobilize the antibody in Fig. 4b, respectively. We can observe that the peak output voltage of the sensor is about −55 μV when the antibody is immobilized by AuNPs; the peak output voltage is about −40 μV when the antibody is immobilized by UiO-66-NH_2; and the peak output voltage increases to −30 μV when the antibody is immobilized by the composite material. The response differences are attributed to the differences of specific surface area. On one hand, more AuNPs can connect with amino groups of UiO-66-NH_2 for signal amplification. On the other hand, the carboxyl groups on the surface of UiO-66-NH_2 can also be the binding sites of the antibodies. Therefore, the nanomaterials improve the sensor sensitivity by increasing antibody load.

During the whole experiment, the thickness of PVDF film we used was 28 μm (a fixed product parameter). Actually, modifier quantity on the PVDF film surface can affect sensitivity of this sensor. As one of optimization experiments, we controlled modifier quantity with the modifier concentration for the sensitivity control of this sensor. The experimental results are shown in Figs. 4c and d. The response of microcantilever sensor in the range of UiO-66-NH_2 concentration of 1-9 mg/mL was studied. As can be seen from Fig. 4c, with the increase of UiO-66-NH_2 concentration, the voltage output extreme value of the microcantilever continues to increase. This is because the larger the antibody fixation amount on the surface of the microcantilever, the more antigen binding sites, resulting in the increase of the stress of the microcantilever, that is, the output voltage value will also increase. When the concentration of UiO-66-NH_2 reaches 7 mg/mL, the voltage output extreme value of the microcantilever reaches the maximum. If the concentration of UiO-66-NH_2 continues to increase, the voltage output value will not increase, which may be due to the saturation of the antibody fixed per unit area. Therefore, the optimal concentration of UiO-66-NH_2 is 7 mg/mL. In addition, the activation time of EDC/NHS also has a certain effect on the immune response. In this experiment, the relationship between different activation time and the voltage output extreme value of microcantilever sensor was investigated. The activation times were 30, 40, 50, 60 and 70 min, respectively. It can be seen that the sensor voltage increases with the increase of activation time (Fig. 4d). When the activation time reaches 60 min, the voltage output value of the microcantilever reaches the maximum value. If the activation time continues to increase, the peak voltage output of the microcantilever beam will not increase. Therefore, the optimal activation time for EDC/NHS is 60 min.

As shown in Fig. 5a, under the optimum conditions, the peak voltage signal of microcantilever sensor increased with increasing concentration of H9N2 antigen. The H9N2 microcantilever sensor showed a wide linear range from 100 ng/mL to 1000 ng/mL with a low detection limit of 2.9 ng/mL and a correlation coefficient of 0.991, as shown in Fig. 5b. The detection limit is calculated according to $3\sigma/S$, (σ represents the standard deviation of the blank signal, and S represents the slope of the calibration curve). In addition, this method was compared with the previous immunosensors for virus detection, and shown in Table S2 (Supporting information). We found that the self-driven and self-sensing microcantilever sensor we constructed has high sensitivity; in addition, it also has the advantages of simple operation and low price (< 300 CNY), which is not available in other immunosensors advantage.

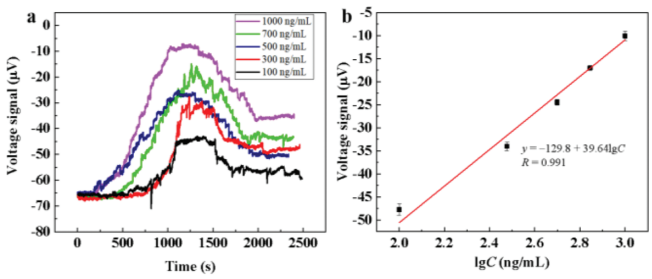

Fig. 5. (a) Voltage response towards different concentrations of AIV H9N2. (b) Calibration curve for H9N2 AIV determination.

To determine the selectivity of the method for AIV H9N2, newcastle disease virus (NDV), reticuloendoth eliosis virus (REV), avian leukosis virus (ALV), goose parvoviruse (GPV), and chicken anaemia virus (CAV) were selected as interferers. As shown in Fig. S4 (Supporting information), the interference group (500 ng/mL) did not cause significant voltage signal enhancement, and its voltage value was close to that of the blank group. The voltage signal was significantly enhanced only in the presence of H9N2 virus (500 ng/mL), indicating that the method has good selectivity.

To evaluate the reproducibility of this sensor, five microcantilever immunosensors prepared from the same batch were used to detect H9N2 at 300 ng/mL. The relative standard deviation (RSD) of the five sensors was 4.2%, indicating that the designed microcantilever immunosensor has good reproducibility. Besides, we also investigated the stability of the sensor. The prepared immunosensor was stored in the refrigerator at 4 °C, and the signal intensity was still maintained at 85.9% of the original 300 ng/mL after three weeks. The above tests show that the sensor has satisfactory stability.

In this work, a new type of microcantilever sensor with self-driving and self-sensing properties was constructed through piezoelectric materials. H9N2 antibody was successfully immobilized on the gold surface of the microcantilever through nanomaterials, and the concentration of H9N2 antigen and its voltage were established. The value output relationship realizes the detection of H9N2. The sensor has the advantages of high sensitivity, simple operation and fast response. Compared with the traditional optical detection method, the microcantilever sensor detection technology using the electrical principle not only saves the high cost of optical equipment, but also can use the self-built detection device to monitor the specific interaction process of H9N2 in real time. Therefore, the microcantilever sensor, as a new detection platform, has broad application prospects in the research of tumor markers and biomolecules detection process and their interaction force.

Declaration of competing interest

The authors declare that they have no known competing financial interests or personal relationships that could have appeared to influence the work reported in this paper.

Acknowledgments

The authors acknowledge the financial support from National Natural Science Foundation of China (No. 22102141), the Priority Academic Program Development of Jiangsu Higher Education Institutions (PAPD), Nature Science Foundation of Jiangsu Province No. BK20190905, and Project for Science and Technology of Yangzhou (No. YZ2020067). H. Chong thanks Dr Aijian Qin and Hongxia Shao to provide the H9N2 antibody and antigen reagents, and also acknowledges the open funds of the Ministry of Education Key Lab for Avian Preventive Medicine (No. YF202020).

Supplementary materials

Supplementary material associated with this article can be found, in the online version, at doi:10.1016/j.cclet.2022.07.043.

References

[1] F.W. Luo, C. Long, Z. Wu, et al., Sens. Actuators B: Chem. 310 (2020) 127831.
[2] C.H. Zhou, Y.M. Long, B.P. Qi, D.W. Pang, Z.L. Zhang, Electrochem. Commun. 31 (2013) 129–132.
[3] C.H. Zhou, Y. Shu, Z.Y. Hong, D.W. Pang, Z.L. Zhang, Chem. Asian J. 8 (2013) 2220–2226.
[4] X.L. Peng, G. Luo, Z. Wu, et al., ACS Appl. Mater. Interfaces 11 (2019) 41148–41156.
[5] B Zhang, H Zhang, M Zhong, et al., Chin. Chem. Lett. 31 (2020) 133–135.
[6] F Shi, J. Xu, Z. Hu, et al., Chin. Chem. Lett. 32 (2021) 3185–3188.
[7] X.J. Chen, Y.G. Pan, H.Q. Liu, et al., Biosens. Bioelectron. 79 (2016) 353–358.
[8] D.K. Agarwal, A. Kushagra, M. Ashwin, A.S. Shukla, V. Palaparthy, Nanotechnology 31 (2020) 115503.
[9] L.S. Huang, Y. Pheanpanitporn, Y.K. Yen, et al., Biosens. Bioelectron. 59 (2014) 233–238.
[10] U. Sungkanak, A. Sappat, A. Wisitsoraat, C. Promptmas, A. Tuantranont, Biosens. Bioelectron. 26 (2010) 784–789.
[11] K. Nieradka, T.P. Gotszalk, G. Schroeder, Sens. Actuators B: Chem. 170 (2012) 172–175.
[12] K.M. Hansen, T. Thundat, Methods 37 (2005) 57–64.
[13] D. Xu, L. Liu, J. Guan, et al., Microchim. Acta 181 (2014) 403–410.
[14] S. Maruyama, Y.J. Choi, K. Takahashi, K. Sawada, Sensor. Mater. 31 (2019) 2895–2906.
[15] P.M. Kosaka, V. Pini, J.J. Ruz, et al., Nat. Nanotechnol. 9 (2014) 1047–1053.
[16] L.H. Zeng, M.Z. Wang, H. Hu, et al., ACS Appl. Mater. Interfaces 5 (2013) 9362–9366.
[17] C. Luan, X. Yao, C. Liu, L. Lan, J. Fu, Carbon 140 (2018) 100–111.
[18] S. Wang, D.D.L. Chung, Carbon 44 (2006) 2739–2751.
[19] J. Zhou, P. Li, S. Zhang, et al., Microelectron. Eng. 69 (2003) 37–46.
[20] S. Faegh, N. Jalili, S. Sridhar, Sensors 13 (2013) 6089–6108.
[21] S. Faegh, N. Jalili, O. Yavuzcetin, et al., J. Appl. Phys. 113 (2013) 224905.
[22] J Chen, J Liu, X Chen, et al., Chin. Chem. Lett. 30 (2019) 1575–1580.
[23] J Li, W Li, Y Rao, et al., Chin. Chem. Lett. 32 (2021) 150–153.
[24] L. Liu, L. Zhang, F. Wang, et al., Nanoscale 11 (2019) 7554–7559.
[25] C. Wang, L. Liu, X. Liu, et al., Sens. Actuators B: Chem. 307 (2020) 127619.
[26] A. Ravalli, G.P. dos Santos, M. Ferroni, et al., Sens. Actuators B: Chem. 179 (2013) 194–200.
[27] D. Lee, EH. Kim, M. Yoo, et al., Appl. Phys. Lett. 90 (2007) 113107.
[28] J. Yuan, X. Chen, H. Duan, et al., Microchim. Acta 187 (2020) 640.
[29] N. Li, X. Huang, D. Sun, et al., Microchim. Acta 185 (2018) 543.
[30] S. Li, X. Wang, Q. He, et al., Chin. J. Catal. 37 (2016) 367–377.
[31] P. Ling, J. Lei, L. Jia, H. Ju, Chem. Commun. 52 (2016) 1226–1229.
[32] L. Yin, Y. Wang, R. Tan, H. Li, Y. Tu, Microchim. Acta 188 (2021) 53.